SLOT RESONATORS FOR CHARACTERIZATION OF DIELECTRICS AT MICROWAVE FREQUENCIES

H. G. Akhavan and D. Mirshekar-Syahkal
Department of Electronic Systems Engineering
University of Essex
Colchester, Essex CO4 3SQ, UK

INTRODUCTION

Open planar resonators like single and stacked microstrip resonators were used in the past for the measurement of dielectric constants and thicknesses of lossy and lossless dielectrics at microwave frequencies [1-3]. With a large width, the microstrip resonator effectively acts as a planar antenna in which case the fringing field is significant for the two slots at the two ends of the resonator and the resonator Q-factor is low. One of the limitations of the microstrip resonator is its spatial resolution which is determined by the size of the resonator. It is envisaged that this problem can be overcome by the use of planar slot resonators, Fig.1. Furthermore, compared to the microstrip-fed microstrip resonator, a microstrip-fed planar slot resonator would provide a better isolation between the feed and the material under test.

In this paper, we initially present the use of the microstrip-fed slot resonator for measuring dielectric constants of materials. The dielectric under test can be liquid or solid, but must have a flat surface. To measure the dielectric constant, the resonator is brought into contact with the dielectric surface and the shifts in its resonant frequency, bandwidth and input impedance at the feed, are used to determine the characteristics of the dielectric. Since changes in these parameters are also dependent on the thickness of the dielectric, experimental results are presented to show the effect of the dielectric thickness.

Like many NDE techniques, a precise determination of the complex permittivity of a dielectric with the planar slot resonator depends on the accuracy of the mathematical modeling or experimental calibrations available for the interpretation of measurements. For this purpose, a general and accurate pseudo-numerical technique for the analysis of the slot resonator loaded with a dielectric is also presented. Theoretical results for an example planar slot resonator when applied to different dielectrics are given.

PLANAR SLOT RESONATOR

The schematic diagram of the planar slot resonator fed by the microstrip line together with a simple equivalent circuit for this structure is given in Fig.1.a-b. As seen in Fig.1.a, the micrstrip line is coupled to the slot at its center. The length of the open-ended microstrip stub is chosen such that maximum coupling is achieved between the feeder and the slot at a particular frequency. To be compatible with standard detecting systems, the feed line impedance is designed to be 50 Ohm. At the fundamental resonant mode, the impedance of the resonator as measured at the center of the slot is very high (about 400 Ohm) and is virtually equal to the radiation resistance of the slot [4]. As a result, a large mismatch would exist between the feed line and the resonator. By an appropriate choice of the length of the open-ended microstrip stub, the mismatch can be reduced to some extent, but a satisfactory

Review of Progress in Quantitative Nondestructive Evaluation, Vol 16
Edited by D.O. Thompson and D.E. Chimenti, Plenum Press, New York, 1997

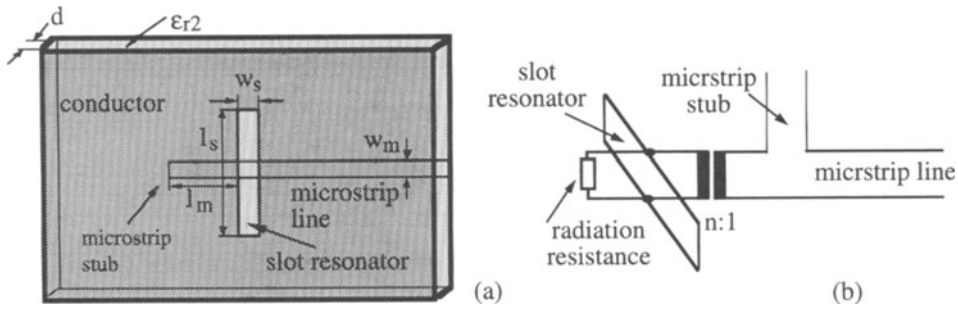

Fig.1 (a) A slot resonator and (b) its equivalent circuit.

match of the resonator to the feed line requires an extra matching circuit. However, as far as the dielectric measurement is concerned, a highly matched system is not necessary. As will be shown later, the matching condition is a function of the dielectric under test and is in fact monitored to characterize dielectrics.

To determine the permittivity of a dielectric, the planar slot resonator is pressed against the test specimen and the resonant frequency and the reflection coefficient (which is directly related to the input impedance) are compared against those of the unloaded resonator. The results are then translated into permittivity by means of a set of curves obtained experimentally or theoretically. The changes in the resonant frequency are due to the interaction of the electric field of the resonator with the material under test. Therefore, for an accurate measurement, care must be taken to keep the interacting field (near field) within the specimen. In other words, the specimen must have a sufficiently large thickness. In Fig.2, the result of an experiment carried out to determine the thickness criterion for perspex is shown. In this experiment, a slot resonator was discretely loaded with perspex sheets, each of 2 mm thickness. As can be seen in Fig.2, for the particular resonator used, the resonant frequency becomes constant (tolerating an error of 0.6%) for thicknesses greater than 12 mm. This figure is not universal and depends on the resonator dimensions and the dielectric under test.

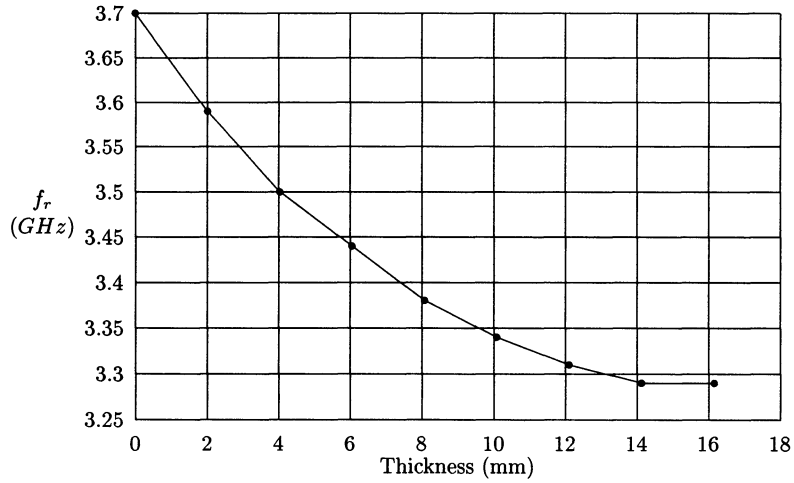

Fig.2 The effect of dielectric thickness on the resonant frequency of a slot resonator. The dielectric is perspex and the resonator specifications are l_s=44 mm, w_s=3 mm, w_m=4.8 mm, l_m=25 mm, d=1.59 mm and ε_{r2}=2.2.

As alluded in the previous paragraph, the inversion of the measurement data (the resonant frequency and return-loss) into complex permittivity can be accomplished using inversion curves obtained experimentally. However, this is appropriate and economical when there is a limited range of dielectrics. When a wide range of dielectrics is to be dealt with, acquiring the suitable dielectric specimens and repeating the experiments in order to set up the inversion curves can be very costly, time consuming and at times can be impossible. Therefore, the inversion should be based on theoretical data. This point was the impetus behind the development of the theoretical analysis technique outlined in the next section.

THEORETICAL MODELING

The dielectric loaded slot resonator shown in Fig.3.a can be analyzed using different mathematical methods. In this work, the analysis is based on the spectral domain technique (STD) [5]. This technique is pseudo-numerical and, hence, very efficient computationally. The main assumptions used in order to be able to apply the SDT are as follows: the ground plane and the dielectrics extend to infinity in the x and y direction, the ground plane has negligible thickness (ie: there is no air gap between the resonator substrate and the dielectric under test) and the dielectric under test has an infinite thickness.

A detailed account of the STD applied to planar circuits can be found in [5]. In this work, initially the equivalence principle is invoked [4, 6]. The slot is replaced by a perfect conductor together with equal surface magnetic currents of opposite directions just above and below the conductor, Fig.3.b. Since the widths of the slot and the microstrip line are small, only the x-directed electric current, J_x, along the microstrip line and the y-directed magnetic current, M_y, along the slot, are taken into account in the analysis. Considering these currents, the integral equations of the problem are

$$E_{xm}(x,y,0) = \iint_{S_m} G_{xx}^{EJ} J_x dx_0 dy_0 + \iint_{S_s} G_{xy}^{EM} M_y dx_0 dy_0 \tag{1.a}$$

$$J_{xs}(x,y,d) = \iint_{S_m} G_{yx}^{HJ} J_x dx_0 dy_0 + \iint_{S_s} G_{xy}^{HM} M_y dx_0 dy_0 \tag{1.b}$$

where $E_{xm}(x, y, 0)$ is the electric field at the microstrip interface, $J_{xs}(x, y, d)$ is the electric current at the slot interface, S_m and S_s are the surfaces of the microstrip line and the slot respectively. In (1), G_{xx}^{EJ} and G_{yx}^{HJ} are the dyadic Green's function components due to a unit x-directed current at $(x_0, y_0, 0)$, and G_{xy}^{EM} and G_{xy}^{HM} are the dyadic Green's function components due to a unit y-directed magnetic current at (x_0, y_0, d).

Using the two-dimensional Fourier transform with spectral parameters k_x and k_y, each of the Green's function components can be expressed in terms of its spectra. For example

$$G_{xx}^{EJ}(x,y|x_0,y_0) = \int_{-\infty}^{+\infty}\int_{-\infty}^{+\infty} \tilde{G}_{xx}^{EJ}(k_x,k_y) e^{jk_x(x-x_0)} e^{jk_y(y-y_0)} dk_x dk_y \tag{2}$$

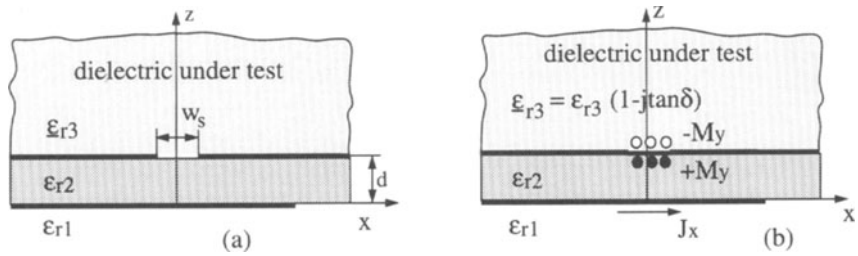

Fig.3 (a) The slot resonator applied to a dielectric and (b) the equivalent problem.

The expressions for the spectral domain forms of the Green's function components are

$$\tilde{G}_{xx}^{EJ} = -j\frac{\sin\gamma_2 d}{\omega\varepsilon_0\beta^2}\left[\frac{\gamma_1\gamma_2 k_x^2}{T_m} + \frac{k_0^2 k_y^2}{T_e}\right], \quad \tilde{G}_{yx}^{HJ} = -\tilde{G}_{xy}^{EM} = \frac{1}{\beta^2}\left[\frac{\gamma_1\varepsilon_{r2}k_x^2}{T_m} + \frac{\gamma_2 k_y^2}{T_e}\right] \tag{3.a}$$

$$\tilde{G}_{yy}^{HM} = \frac{j}{\omega\mu_0}\left[\frac{j(\gamma_2\cos\gamma_2 d + j\gamma_1\varepsilon_{r2}\sin\gamma_2 d)(\varepsilon_{r2}k_0^2 - k_y^2)}{\gamma_2 T_m} - \frac{jk_y^2\gamma_2(\varepsilon_{r2}-1)}{T_e T_m} - \frac{(\underline{\varepsilon}_{r3}k_0^2 - k_y^2)}{j\gamma_3}\right] \tag{3.b}$$

where

$$T_m = \varepsilon_{r2}\gamma_1\cos\gamma_2 d + j\gamma_2\sin\gamma_2 d, \quad T_e = \gamma_2\cos\gamma_2 d + j\gamma_1\sin\gamma_2 d \tag{3.c}$$

$$\gamma_1^2 = (k_0^2 - \beta^2)^2, \quad \gamma_2^2 = (\varepsilon_{r2}k_0^2 - \beta^2)^2, \quad \gamma_3^2 = (\underline{\varepsilon}_{r3}k_0^2 - \beta^2)^2 \tag{3.d}$$

$$\beta^2 = k_x^2 + k_y^2, \; k_0^2 = \omega^2\mu_0\varepsilon_0, \quad \underline{\varepsilon}_{r3} = \varepsilon_{r3}(1 - j\tan\delta_3) \tag{3.e}$$

These are obtained by solving the wave equation in the Fourier domain subject to appropriate boundary conditions [3, 5, 6].

The coupled integral equations in (1) can be solved using the method of moments [5]. Far from the slot, the electric current, J_x, on the microstrip line can be assumed as a combination of the incident current, J_x^{inc} and the reflected current, J_x^{ref}. The reflected current is related to the incident one through a reflection coefficient, R. Around the slot, the current distribution is a combination of the previous two currents and a perturbation current which can be approximated with a set of piece-wise sinusoidal basis functions, $f_n(x)$. Therefore, the current along the microstrip line can be written as

$$J_x = J_x^{inc} + J_x^{ref} + \sum_{n=1}^{N} I_n f_n(x) \tag{4}$$

The above expression is based on the assumption that J_x does not change with y which is valid for a microstrip line with a small width. The magnetic current, M_y, along the slot can be approximated with a set of piece-wise sinusoidal basis functions, $s_m(y)$. In this case the current is expressed as

$$M_y = \sum_{m=1}^{M} E_m s_m(y) \tag{5}$$

Again, it is assumed that the slot width is very small and hence, M_y is not a function of x. In (4) and (5), I_n and E_m as well as R (implicit in the reflected current) are unknown.

Substituting J_x and M_y in (1) and enforcing the boundary conditions that the electric field must be zero on the strip and the tangential magnetic field must be continuous at the two sides of the slots, the following integral equations result

$$\iint_{S_m} G_{xx}^{EJ}[J_x^{inc} + J_x^{ref} + \sum_{n=1}^{N} I_n f_n(x_0)]dx_0dy_0 + \iint_{S_s} G_{xy}^{EM}[\sum_{m=1}^{M} E_m s_m(y_0)]dx_0dy_0 = 0 \tag{6.a}$$

$$\iint_{S_m} G_{yx}^{HJ}[J_x^{inc} + J_x^{ref} + \sum_{n=1}^{N} I_n f_n(x_0)]dx_0dy_0 + \iint_{S_s} G_{xy}^{HM}[\sum_{m=1}^{M} E_m s_m(y_0)]dx_0dy_0 = 0 \tag{6.b}$$

The coupled equations in (6) are solved using the Galerkin method [5]. In this method of moments, the testing functions are the same as the basis functions, leading to a matrix equation

$$\begin{bmatrix} & [I_n] & \\ [Z] & R & \\ & [E_m] & \end{bmatrix} = [V] \tag{7}$$

whose solution yields the unknown expansion coefficients I_n, E_m and R. In (7), [V] is a known matrix whose elements are the inner products of the incident wave with the testing functions. The elements of the [Z] matrix can be expressed, in general form, as follows:

$$Z_{ij} = \int_{-\infty}^{+\infty}\int_{-\infty}^{+\infty} \tilde{G}_{**}^{**}(k_x,k_y)F_{ij}(k_x,k_y)dk_x dk_y \tag{8}$$

where '*' refers to sub- and super-scripts of the Green's function components stated in (3) and $F_{ij}(k_x, k_y)$ is the result of testing the basis functions with the basis functions in the Fourier domain. To evaluate the double integral in (8), it is transformed from k_x-k_y plane to polar plane α-β using the well-know transformation

$$k_x = \beta\cos\alpha \qquad k_y = \beta\sin\alpha \tag{9}$$

In the new plane, the integral appears as

$$I = \int_{C_\beta}\int_{0}^{2\pi} \frac{H(\alpha,\beta)}{T_m T_e}\beta d\alpha d\beta \tag{10}$$

where C_β is the path of integration. To choose a correct path, the two valued function γ_i (i=1, 2, 3) in (3) and the location of the singularities must be taken into consideration. The singularities, which are the roots of T_e and T_m in (10), represent the surface waves associated with the resonator substrate (layer 2 in Fig.3).

RESULTS

The modeling reported in the previous section was employed to analyze the behavior of a slot resonator when applied to different lossless ($\tan\delta_3$=0) dielectric specimens. The resonator has the following specifications: l_s=44 mm, w_s=3 mm, w_m=4.8 mm, l_m=25 mm, d=1.59 mm and ε_{r2}=2.2. For the cases analyzed, the results of the return losses, RL, at the feed line are depicted in Fig.4. Amongst these results are the experimental and theoretical values of RL of the unloaded resonator (ie: resonator in air). As can be seen, the theory can predict the measurement very closely. Furthermore, Fig.4 shows that both the resonant frequency and the matching condition vary with the dielectric constant of the material under test. The resonant frequency tends to decrease with increasing the dielectric constant whereas the matching condition is a more complex function of this parameter.

In Fig.5, the effects of dielectric losses on RL are shown for a particular dielectric (ε_{r3}=2) by increasing its loss tangent ($\tan\delta$) from zero. As can be seen in Fig.5, small losses ($\tan\delta$ <0.2) do not perturb the resonant frequency of the resonator significantly. In contrast, the mismatch seems to be sensitive to the losses and increases with increasing the loss-tangent. For large losses both the frequency and the return-loss are strongly affected. In all the above cases, the bandwidth increases by increasing the dielectric loss.

From the results in Figs.4 and 5, it can be concluded that two sets of information for the characterization of a dielectric with low losses are required. A curve is needed to relate the

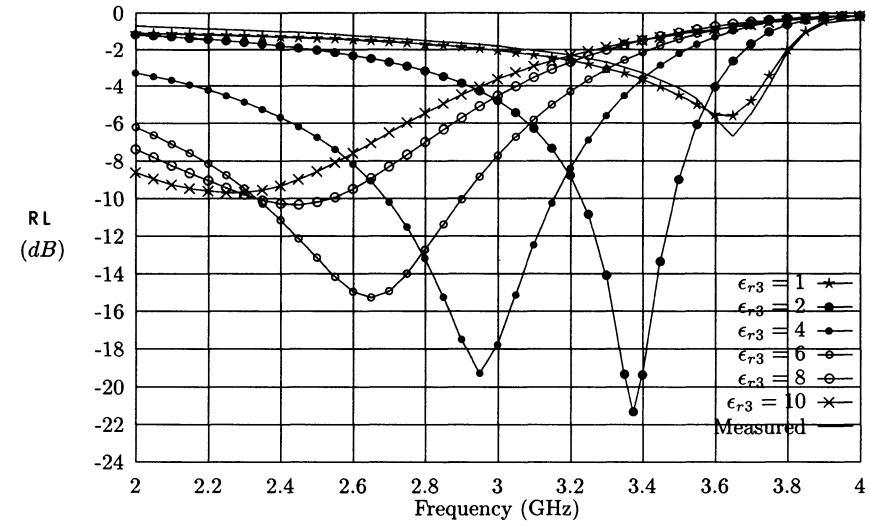

Fig.4 The return-losses of the resonator when applied to different lossless dielectrics.

dielectric constant to the shift in the resonant frequency of the unloaded resonator and another curve is required to relate the return-loss to the loss-tangent for a particular dielectric constant. From the first curve, the dielectric constant of the material is obtained and from the second curve appropriate for the dielectric constant found, the loss-tangent is estimated. Example of such curves are shown in Figs.6.a and 6.b. It should be emphasized again that these curves are appropriate for the characterization of dielectrics with very large (ideally infinitely large) thicknesses. When the thickness of the dielectric is not sufficiently large, the radiation resistance (Fig.1.b) is affected and the effect is reflected in the return-loss (RL), leading to a gross error in the determination of the loss-tangent. For dielectrics with large losses, the inversion is more complex and is currently under investigation.

CONCLUSIONS

The application of the microstrip-fed slot resonator for measuring the permittivities of dielectrics was presented. A technique for the analysis of the slot resonator loaded with a

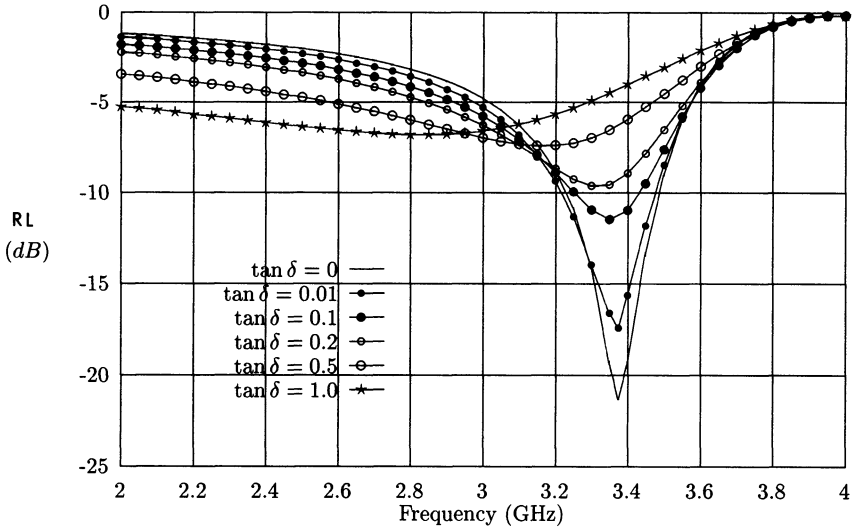

Fig.5 The effect of different losses of a dielectric with ϵ_{r3}=2 on the return-loss of the resonator.

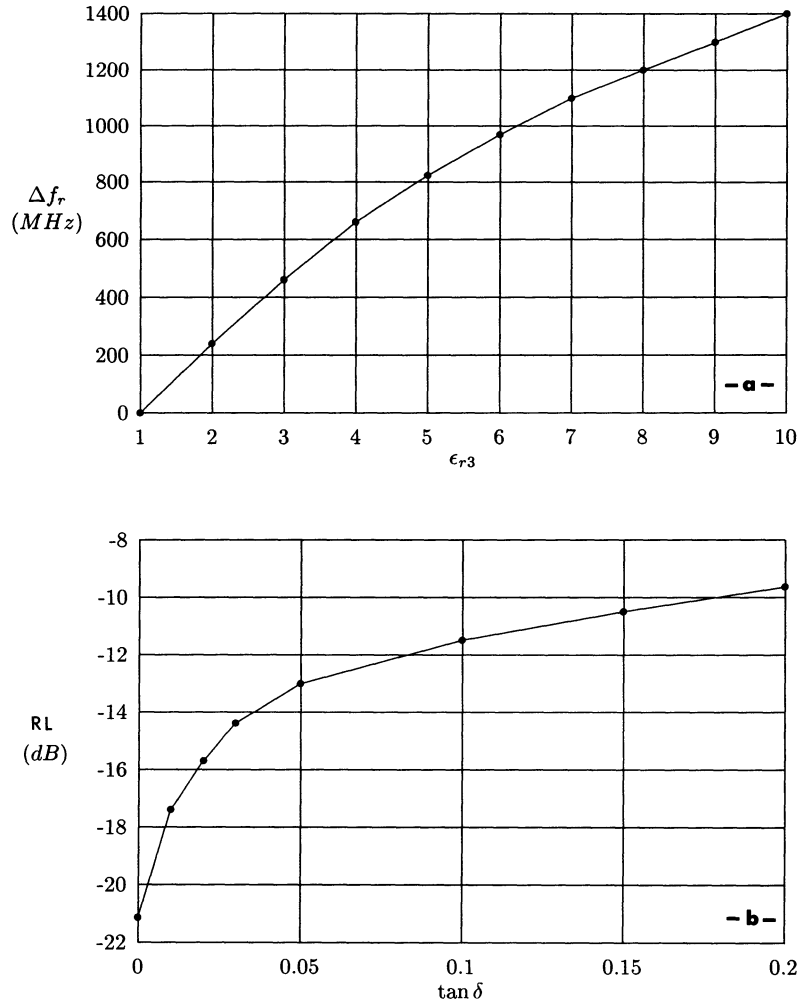

Fig.6 (a) The frequency shift (Δf_r) of the resonator versus the dielectric constant and (b) the return-loss of the resonator versus the loss-tangent of a dielectric with ε_{r3}=2.

lossy dielectric was developed. The technique can be used for the inversion of measurement data. This was demonstrated for low-loss dielectrics.

REFERENCES

1. D. Shimin, IEEE Trans. Microwave Theory Tech., Vol. MTT-34, p. 923 (1986).
2. R. Zoughi and T. Vaughan, in *Review of Progress in Quantitative Non-destructive Evaluation,* Vol. 9, eds. D. O. Thompson and D. E. Chimenti (Plenum Press, New York, 1990), p. 1621.
3. H. R. Hassani and D. Mirshekar-Syahkal, in *Review of Progress in Quantitative Non-destructive Evaluation,* Vol. 11, *op. cit.* (1992), p. 521.
4. C. A. Balanis, *Antenna Theory, Analysis and Design,* (Harper and Row, New York, 1982).
5. D. Mirshekar-Syahkal, *Spectral Domain Technique for Microwave Integrated Circuits,* (John Wiley and Sons, New York, 1990).
6. A. B. Kouki, R. Mittra and C. H. Chan, IEEE Trans. Microwave Theory Tech., Vol. MTT-41, p. 1356 (1993).